



**HAL**  
open science

**Coexistence of closed orbit and quantum interferometer  
with the same cross section in the organic metal  
(ET)<sub>4</sub>(H<sub>3</sub>O)[Fe(C<sub>2</sub>O<sub>4</sub>)<sub>3</sub>].C<sub>6</sub>H<sub>4</sub>Cl<sub>2</sub>: Persistence of SdH  
oscillations above 30 K**

David Vignolles, Alain Audouard, Vladimir N. Laukhin, Enric Canadell,  
Tatyana G. Prokhorova, Eduard B. Yagubskii

► **To cite this version:**

David Vignolles, Alain Audouard, Vladimir N. Laukhin, Enric Canadell, Tatyana G. Prokhorova, et al.. Coexistence of closed orbit and quantum interferometer with the same cross section in the organic metal (ET)<sub>4</sub>(H<sub>3</sub>O)[Fe(C<sub>2</sub>O<sub>4</sub>)<sub>3</sub>].C<sub>6</sub>H<sub>4</sub>Cl<sub>2</sub>: Persistence of SdH oscillations above 30 K. 2009. hal-00406520v1

**HAL Id: hal-00406520**

**<https://hal.science/hal-00406520v1>**

Preprint submitted on 22 Jul 2009 (v1), last revised 7 Oct 2009 (v2)

**HAL** is a multi-disciplinary open access archive for the deposit and dissemination of scientific research documents, whether they are published or not. The documents may come from teaching and research institutions in France or abroad, or from public or private research centers.

L'archive ouverte pluridisciplinaire **HAL**, est destinée au dépôt et à la diffusion de documents scientifiques de niveau recherche, publiés ou non, émanant des établissements d'enseignement et de recherche français ou étrangers, des laboratoires publics ou privés.

# Indications for the coexistence of closed orbit and quantum interferometer with the same cross section in the organic metal $\beta''$ -(ET)<sub>4</sub>(H<sub>3</sub>O)[Fe(C<sub>2</sub>O<sub>4</sub>)<sub>3</sub>]·C<sub>6</sub>H<sub>4</sub>Cl<sub>2</sub>: Persistence of Shubnikov-de Haas oscillations above 30 K

David Vignolles<sup>1</sup>, Alain Audouard<sup>1</sup>, Vladimir N. Laukhin<sup>2,3</sup>, Enric Canadell<sup>3</sup>, Tatyana G. Prokhorova<sup>4</sup>, and Eduard B. Yagubskii<sup>4</sup>

<sup>1</sup> Laboratoire National des Champs Magnétiques Intenses (UPR 3228 CNRS, INSA, UJF, UPS) 143 avenue de Rangueil, F-31400 Toulouse, France.

<sup>2</sup> Institució Catalana de Recerca i Estudis Avançats (ICREA), 08010 Barcelona, Spain.

<sup>3</sup> Institut de Ciència de Materials de Barcelona (ICMAB - CSIC), Campus UAB, 08193 Bellaterra, Catalunya, Spain.

<sup>4</sup> Institute of Problems of Chemical Physics, Russian Academy of Sciences, 142432 Chernogolovka, Moscow oblast, Russia.

Received: July 22, 2009/ Revised version: date

**Abstract.** Shubnikov-de Haas (SdH) and de Haas-van Alphen (dHvA) oscillations spectra of the quasi-two dimensional charge transfer salt  $\beta''$ -(ET)<sub>4</sub>(H<sub>3</sub>O)[Fe(C<sub>2</sub>O<sub>4</sub>)<sub>3</sub>]·C<sub>6</sub>H<sub>4</sub>Cl<sub>2</sub> have been investigated in pulsed magnetic fields up to 54 T. The data reveal three basic frequencies  $F_a$ ,  $F_b$  and  $F_{b-a}$ , which can be interpreted on the basis of three compensated closed orbits at low temperature. However a very weak thermal damping of the Fourier component  $F_b$ , with the highest amplitude, is evidenced for SdH spectra above about 6 K. As a result, magnetoresistance oscillations are observed at temperatures higher than 30 K. This feature, which is not observed for dHvA oscillations, is in line with quantum interference, pointing to a Fermi surface reconstruction in this compound.

**PACS.** 71.18.+y Fermi surface: calculations and measurements; effective mass, g factor – 71.20.Rv Polymers and organic compounds – 72.15.Gd Galvanomagnetic and other magnetotransport effects

## 1 Introduction

The family of quasi-two-dimensional (q-2D) charge transfer salts  $\beta''$ -(ET)<sub>4</sub>(A)[M(C<sub>2</sub>O<sub>4</sub>)<sub>3</sub>]-Solv (where ET stands for bis-ethylenedithio-tetrathiafulvalene, A is a monovalent cation, M is a trivalent cation and Solv is a solvent) have raised great interest for many years [1]. Indeed, even though all the members of this family, denoted as (A, M, Solv) hereafter, are isostructural, it is now established that many different ground-states, including normal metal, charge density wave, superconductivity, and temperature-dependent behaviours can be observed [1].

According to band structure calculations [2], the Fermi surface (FS) of these compounds originates from a hole orbit (labelled  $\odot$  in the following) with an area equal to that of the first Brillouin zone (FBZ). Due to small gap opening, compensated orbits with much smaller area (8.8 % of the FBZ, according to [2]) are formed, as displayed in Fig. 1a. Insofar as the Fermi level is very close to the band extrema at Y [2,3], the actual FS topology can be very sensitive to subtle structural details. Namely, in the case where the  $\odot$  orbits intersect along the  $b^*$  direction, an additional orbit is observed and the FS topology is similar to that of Fig. 1b [4]. Oppositely, if the gap is larger than in the case of Fig. 1a, the electron-type orbits transform into quasi-one dimensional sheets as displayed in Fig. 1c [4]. In addition, FS reconstruction due to phase transition such as density wave condensation can further modify the FS at low temperature. As a matter of fact, depending on the studied compound, Shubnikov-de Haas

(SdH) oscillations spectra have revealed from one to six Fourier components in this family [5,6,7,8,9]. Their frequency are in the range 40 T to 350 T that corresponds to orbits with area ranging from 2 to 18 % of the FBZ area. In most cases, these orbits are compensated, in agreement with band structure calculations. For example, SdH data of (NH<sub>4</sub>, Fe, C<sub>3</sub>H<sub>7</sub>NO) can be interpreted on the basis of three compensated orbits [5], corresponding to the textbook case [10] reported in Fig. 1b where  $a$  and  $b - a$  are hole orbits while  $b$  is an electron orbit. However, more complex SdH spectra, that are strongly dependent on external parameters such as a moderate applied pressure, can also be observed. In addition, significant structural disorder, linked to the size of the solvent molecule, has been reported for many members of this family [11,12,13,14]. Influence of the nature of the solvent molecule on the physical properties, such as the behaviour of the temperature dependence of the resistivity and the occurrence or not of a superconducting ground state, has been considered. In that respect, the temperature-dependent resistivity of (H<sub>3</sub>O, Fe, C<sub>6</sub>H<sub>4</sub>Cl<sub>2</sub>) exhibits a metallic behaviour down to few K, followed by a slight upturn. A magnetoresistance experiment performed on this compound up to 17 T yielded a SdH spectrum involving only two Fourier components [14]. The present paper reports on both magnetoresistance and torque experiments performed up to 54 T on this compound. A third Fourier component is observed. Nevertheless, the main result is the persistence of magnetoresistance oscillations at temperatures above 30 K. This feature, which is not observed in de Haas-van

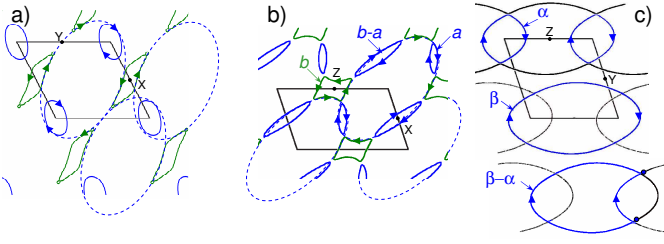


**Fig. 1.** (color on line) Fermi surface of (a)  $\beta''$ -(ET)<sub>4</sub>(NH<sub>4</sub>)[Fe(C<sub>2</sub>O<sub>4</sub>)<sub>3</sub>]-C<sub>3</sub>H<sub>7</sub>NO [2], (b) (BEDO)<sub>4</sub>Ni(CN)<sub>4</sub>·4CH<sub>3</sub>CN [4] and (c) (BEDO)<sub>5</sub>Ni(CN)<sub>4</sub>·3C<sub>2</sub>H<sub>4</sub>(OH)<sub>2</sub> [4]. Ellipses in dashed lines stand for intersecting hole orbits with area equal to that of the First Brillouin zone ( $\odot$  orbits). They lead to three compensated electron ( $b$ ) and hole ( $a$  and  $b - a$ ) orbits in Fig. 1b.  $\odot$  orbits correspond to  $\beta$  orbits of Fig. 1c. The arrows indicate the quasiparticles direction (see text).

Alphen (dHvA) spectra is discussed on the basis of the presence of both a quantum interferometer and a closed orbit with the same area. It points to a FS reconstruction at low temperature.

## 2 Experimental

Magnetoresistance and magnetic torque were measured in pulsed magnetic field up to 54 T with a pulse decay duration of 0.32 s. A one-axis rotating sample holder allowed to change the angle ( $\theta$ ) between the direction of the magnetic field and the  $c^*$  crystal axis. For magnetoresistance measurements, the studied crystal was an elongated hexagonal platelet with approximate dimensions ( $0.4 \times 0.2 \times 0.1$ ) mm<sup>3</sup>, the largest faces being parallel to the conducting  $ab$ -plane. Electrical contacts were made using annealed platinum wires of 20  $\mu$ m in diameter glued

with graphite paste. Alternating current (10  $\mu$ A, 77 Hz and 100  $\mu$ A, 50 kHz for zero-field and magnetoresistance measurements, respectively) was injected parallel to the  $c^*$  direction (interlayer configuration). The explored temperature range was from 1.4 K to 32 K. Magnetic torque measurements were performed with a commercial piezoresistive microcantilever [15] in the temperature range from 1.9 K to 15 K. The crystal size was approximately ( $0.3 \times 0.1 \times 0.07$ ) mm<sup>3</sup>. Variations of the cantilever piezoresistance was measured with a Wheatstone bridge with an ac excitation at a frequency of 63 kHz [16]. A lock-in amplifier with a time constant in the range 30 - 100  $\mu$ s was used to detect the measured signal for magnetoresistance and torque measurements. Discrete Fourier analysis of oscillatory magnetoresistance and torque were performed using Blackman-type window, which is known to avoid secondary lobes.

## 3 Results and discussion

Fourier analysis of the oscillatory part of the magnetoresistance data, obtained with magnetic field normal to the conducting plane ( $\theta = 0^\circ$ ), is displayed in Fig. 2. Four peaks can be identified with frequencies  $F_a = 74 \pm 5$  T,  $F_b = 348 \pm 3$  T,  $F_{b-a} = 272 \pm 5$  T and  $F_{2b} = 699 \pm 5$  T that accounts for the relationship  $F_a + F_{b-a} = F_b$ . The reported uncertainties are deduced from data below 2.2K for various field directions which allow checking that these frequencies follow the  $\cos(\theta)$  dependence expected for a 2D FS (up to  $\theta = 62^\circ$  for the  $b$  component).  $F_a$  and  $F_b$  could correspond to the frequencies  $F_2 \approx 80$  T and  $F_1$

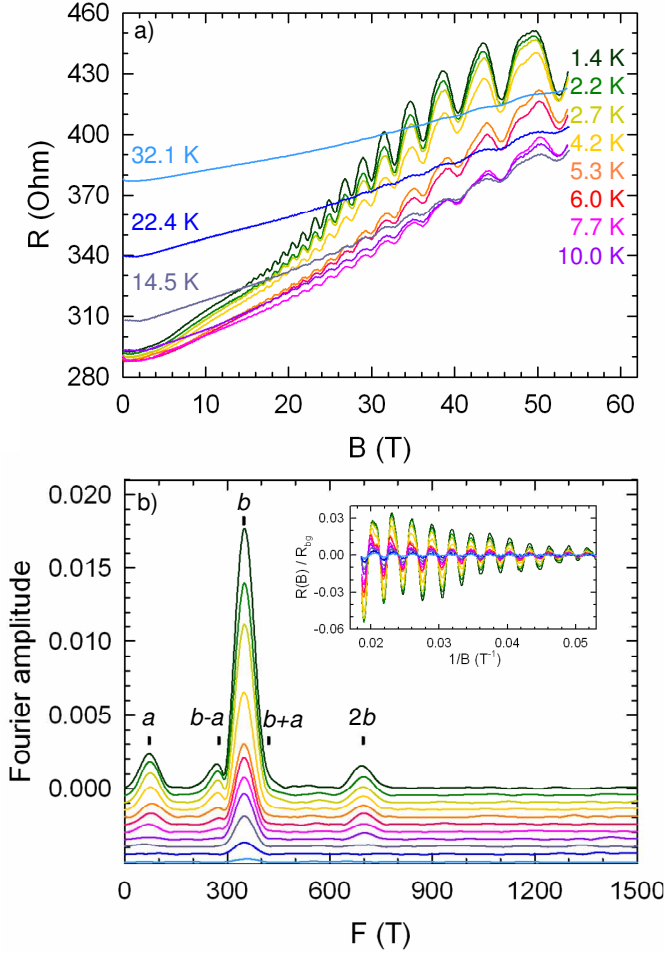


**Fig. 2.** (color on line) (a) Field-dependent interlayer resistance of  $\beta''$ -(ET)<sub>4</sub>(H<sub>3</sub>O)[Fe(C<sub>2</sub>O<sub>4</sub>)<sub>3</sub>]:C<sub>6</sub>H<sub>4</sub>Cl<sub>2</sub> for  $\theta = 0^\circ$ . (b) Fourier analyses deduced from the oscillatory part of the magnetoresistance displayed in the inset. The field range is 18-54 T. Marks are calculated with  $F_a = 74$  T and  $F_b = 348$  T.

$= 376$  T, respectively, reported in [14]. Oscillatory spectra including frequencies  $F_a$ ,  $F_b$  and their combinations have already been observed in few other compounds of the considered family [5,9,17] and interpreted on the basis of a FS similar to that displayed in Fig. 1b [4], taking into account that the respective location of the hole orbits  $a$  and  $b - a$  can be exchanged. It is well known that linear

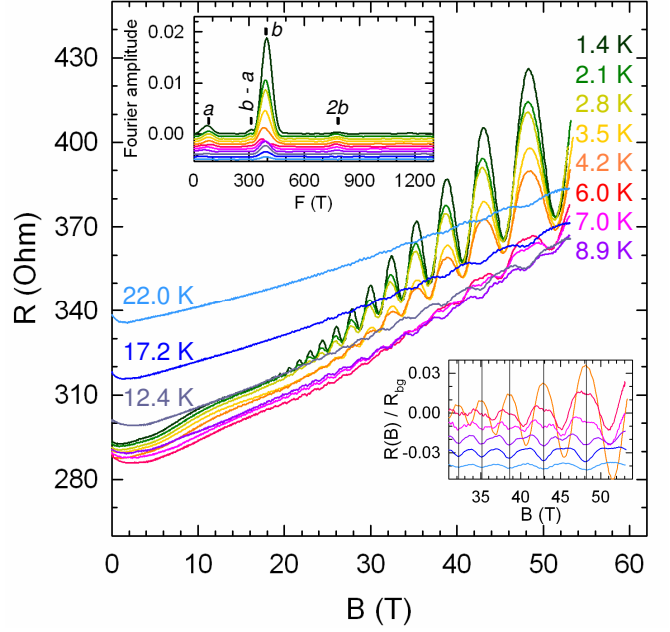


**Fig. 3.** (color on line) Field-dependent interlayer resistance for  $\theta = 27^\circ$ . The upper inset displays corresponding Fourier analyses. Oscillatory part of the magnetoresistance data for temperatures above 4 K are displayed in the lower inset to evidence the change of the Onsager phase factor ( $\gamma_b$ ) discussed in the text. Vertical lines are marks calculated with  $F_b = 390$  T and  $\gamma = 0.1$ .

relationship between frequencies can also be observed for FS topology analogous to Fig. 1c, namely  $F_\alpha + F_{\beta-\alpha} = F_\beta$ , where  $\beta - \alpha$  is a QI path. However, the area of the MB-induced  $\beta$  orbit is equal to that of the FBZ. In the case of the compound of Fig. 1c,  $F_\beta = 3837$  T [18]. Such a frequency value would be close to that expected for the  $\odot$  orbit ( $F_{\odot} = 3975$  T) which is an order of magnitude larger than  $F_b$ .

In the framework of the Lifshits-Kosevich (LK) formula, and assuming that the amplitude of the oscillations is small compared to the background non-oscillating part

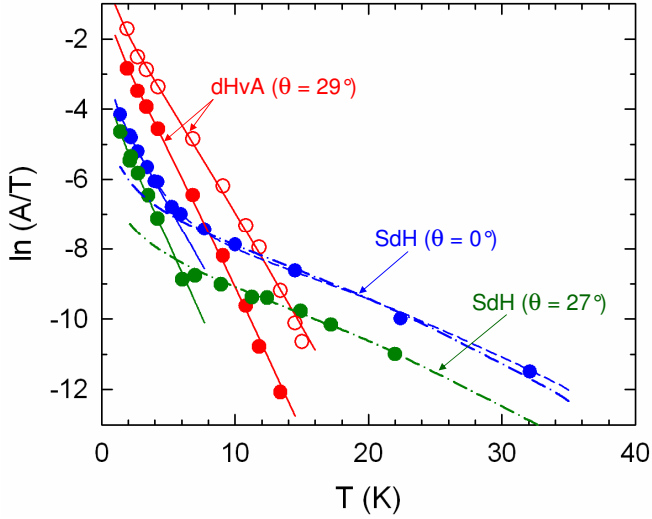


**Fig. 4.** (color on line) Temperature dependence of the amplitude of the  $b$  oscillations for dHvA and SdH data. Empty and solid symbols correspond to a mean field value of 44.6 T and 30 T /  $\cos(\theta)$ . SdH data for  $\theta = 27^\circ$  are shifted down for clarity. Solid and dash-dotted lines are best fits of Eq. 1, assuming the Dingle damping factor is given by Eq. 3 and 7, respectively. In addition, a zero-effective mass is considered for the SdH data in the high temperature range. Dashed line is a best fit to the SdH data for  $\theta = 0^\circ$ , assuming the contributions of closed orbit and quantum interference coexists in all the temperature range covered by the experiments (see text).

of the resistance ( $R_{bg}$ ), the oscillatory magnetoresistance ( $R(B)/R_{bg}$ ) can be accounted for by:

$$\frac{R(B)}{R_{bg}} = 1 + \sum_j A_j \cos[2\pi(\frac{F_j}{B} - \gamma_j)] \quad (1)$$

where  $F_j$  and  $\gamma_j$  are the frequency and the phase factor, respectively, of the Fourier component linked to the orbit  $j$ . The Fourier amplitude is given by  $A_j \propto R_{Tj} R_{Dj} R_{MBj} R_{Sj}$ . The thermal (for a 2D FS), Dingle, magnetic breakdown

(MB) and spin damping factors are respectively given by [19]:

$$R_{Tj} = \frac{\alpha T m_j^*}{B \sinh[\alpha T m_j^* / B]} \quad (2)$$

$$R_{Dj} = \exp[-\alpha T_D m_j^* / B] \quad (3)$$

$$R_{MBj} = \exp(-\frac{t_j B_{MB}}{2B}) [1 - \exp(-\frac{B_{MB}}{B})]^{b_j/2} \quad (4)$$

$$R_{Sj} = \cos(\pi \mu_j / \cos \theta) \quad (5)$$

where  $m_j^*$  is the effective mass normalized to the free electron mass  $m_e$ ,  $T_D = \hbar \tau^{-1} / 2\pi k_B$  is the Dingle temperature,  $\tau^{-1}$  is the scattering rate,  $\mu_j = g^* m_j^*(\theta = 0) / 2$ ,  $g^*$  is the effective Landé factor and  $B_{MB}$  is the MB field. Integers  $t_j$  and  $b_j$  are respectively the number of tunnelling and Bragg reflections that the quasiparticles come up against along their path.

In addition to Fourier analysis, information regarding the oscillatory spectra can also be derived by direct fitting of the LK formula to the field-dependent magnetoresistance. Indeed, direct fitting is useful in order to discern eventual Fourier components with close frequencies and allow for a reliable determination of  $\gamma_j$ . In the high T/B range, and assuming  $t_j = 0$  (see Eq. 4), Eq. 1 can be approximated to:

$$\frac{R(B)}{R_{bg}} = 1 + \sum_j \frac{a_j}{B} \exp(-\frac{B_j}{B}) \cos[2\pi(\frac{F_j}{B} - \gamma_j)] \quad (6)$$

where  $a_j$  is a prefactor. Eq. 6 involves a reduced number of free parameters compared to Eq. 1 since  $B_j \simeq \alpha(T + T_{Dj})m_j^*$ . Its drawback is that, strictly speaking, it is only valid at high temperature, high  $T_D$  and (or) low field. Nevertheless, it is only intended to identify the various Fourier

components entering the data and to derive the parameters  $F_j$  and  $\gamma_j$ . In that respect, Eq. 6 has been successfully used at low temperature and high field for SdH oscillations of (NH<sub>4</sub>, Cr, DMF) under pressure [9] and dHvA oscillations of high- $T_c$  superconductors [16]. In the present case, a very good agreement between frequencies deduced from direct fittings and Fourier analysis is obtained.

Turn on now to the most striking result evidenced in Figs. 2 and 3, namely the persistence of quantum oscillations at temperatures higher than 30 K (up to 22 K at  $\theta = 27^\circ$ ). More insight on this feature can be derived from the field and temperature dependence of the Fourier components observed in the oscillatory part of the magnetoresistance.

As usual, effective masses can be derived from the temperature dependence of the oscillations amplitude through Eq. 2. Data at  $\theta = 0^\circ$  yield  $m_a^* = 0.85 \pm 0.10$  and  $m_{b-a}^* = 1.0 \pm 0.1$  for  $a$  and  $b - a$  Fourier components, respectively. Data for the  $b$  oscillations are displayed in Fig. 4. At low temperature, they yield  $m_b^* = 1.4 \pm 0.2$ . The three effective mass values given above lie in the same range as for other compounds of this family. However, a clear kink can be observed in Fig. 4 as the temperature increases above  $\sim 6$  K. The temperature dependence of the amplitude is much less steep in the high temperature range which accounts for the observation of magnetoresistance oscillations at temperatures as high as 32 K in Fig. 2. The slope of the mass plot would yield  $m^* \simeq 0.35$  at high temperature. However, inelastic collisions cannot be neglected in this range. Indeed, the zero-field interlayer resistance

starts to significantly increase above a few kelvins [14]. As a result, inelastic collisions should account, at least for a part, for the damping of the oscillation amplitude at high temperature. Therefore, the effective mass should be even smaller than the above value. Actually, the data are compatible with a zero effective mass, such as that coming from a symmetric quantum interferometer [20,21,22]. Indeed, assuming the decrease of the  $b$  oscillation amplitude is entirely due to the increase of the inelastic scattering rate  $\tau_i^{-1}$  as the temperature increases and assuming further  $\tau^{-1} = \tau_0^{-1} + \tau_i^{-1}$  and  $\tau_i^{-1} \propto T^2$ , allows to rewrite the Dingle damping factor:

$$R_D = \exp\left[-\frac{\alpha m'}{B}(T_{D0} + \beta T^2)\right] \quad (7)$$

where  $m'$  is the sum of the effective masses linked to each arms of the interferometer [20,21,22] and  $\beta$  is a prefactor. In this case, still assuming a quantum interferometer with a zero effective mass and neglecting MB, reduces the contribution to the  $b$  oscillations amplitude ( $A_b$ ) in the high temperature range to the temperature-dependent  $R_D$  given by Eq. 7. This leads to  $A_b = \exp(p_1 + p_2 T^2)$  where  $p_1 = a_0 - \alpha m' T_{D0}/B$  ( $a_0$  is a constant). Dash-dotted lines in Fig. 4 are best fits to the data in which the product  $\alpha m' \beta$  has been fixed to  $0.085 \text{ TK}^{-2}$ . In agreement with Eq. 7 which assumes a zero-effective mass,  $p_1$  decreases linearly with  $1/B$  (see Fig. 5), even though a zero-effective mass must be regarded as the lowest limit. The value of

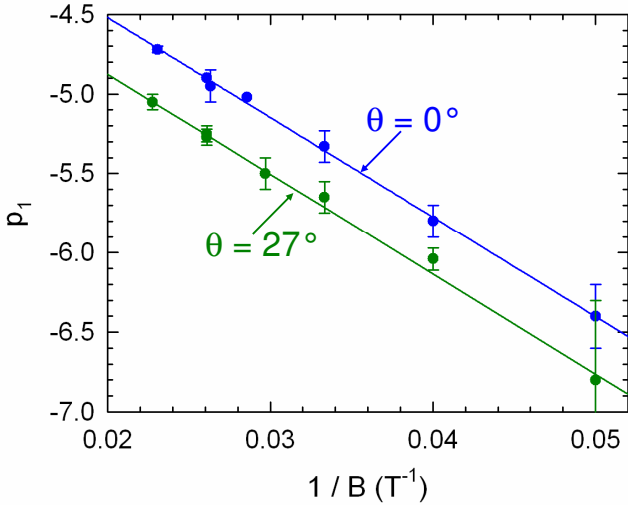


**Fig. 5.** (color on line) Field dependence of the parameter  $p_1 = a_0 - \alpha m' T_{D0}/B$ , deduced from the temperature dependence of the  $b$  oscillations amplitude in the high temperature range for  $\theta = 0^\circ$  and  $27^\circ$ . Solid straight lines are best fits to the data (see text).

the slope, which is negligibly dependent on the value of assumed for  $\alpha m' \beta$ <sup>1</sup>, yields  $m' T_{D0} = 4.3 \pm 0.2$  K.

In the above discussion, it is implicitly assumed that each of the two phenomena (either closed orbit or quantum interference) involved in the  $b$  Fourier component occurs in a separate temperature range or, at the very least, is strongly dominant in the considered temperature range. Oppositely, coexistence of the two phenomena can be directly observed in the temperature range  $\sim 6 - 9$  K for  $\theta = 27^\circ$ . Indeed, in this range, two out of phase oscilla-

<sup>1</sup> A change of the  $\alpha m' \beta$  value, i.e. of  $p_2$ , produces a field-independent shift of the deduced  $p_1$  value. In addition, since a  $T^2$  behaviour of the interlayer resistance is only observed in the range 10-20K, we have checked that assuming  $\tau_i \propto T$  in Eq. 7 still satisfactorily accounts for the data.

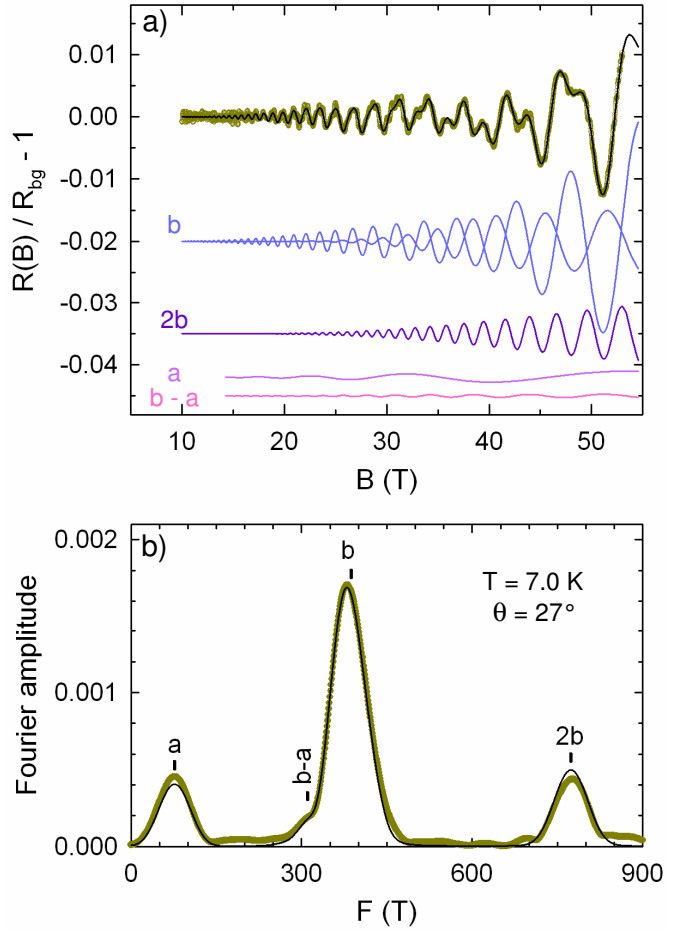


**Fig. 6.** (color on line) (a) Best fit of Eq. 6 (black solid line) to the oscillatory magnetoresistance (yellow solid symbols) at 7.0 K and  $\theta = 27^\circ$ . The various components entering the fittings are shifted from each other by an arbitrary amount. (b) Fourier analysis of the experimental data (yellow solid symbols) and of the best fit (black solid line). The field range is 18 - 53.5 T. Marks correspond to the frequency of the various components entering the fittings. They are obtained with  $F_a = 76.6$  T and  $F_b = 386.9$  T.

tions series with the frequency  $F_b$  can be distinguished in the oscillatory magnetoresistance (see the lower inset of Fig. 3). More insight on this behaviour can be obtained thanks to direct fittings of Eq. 6 that reveal the two  $b$



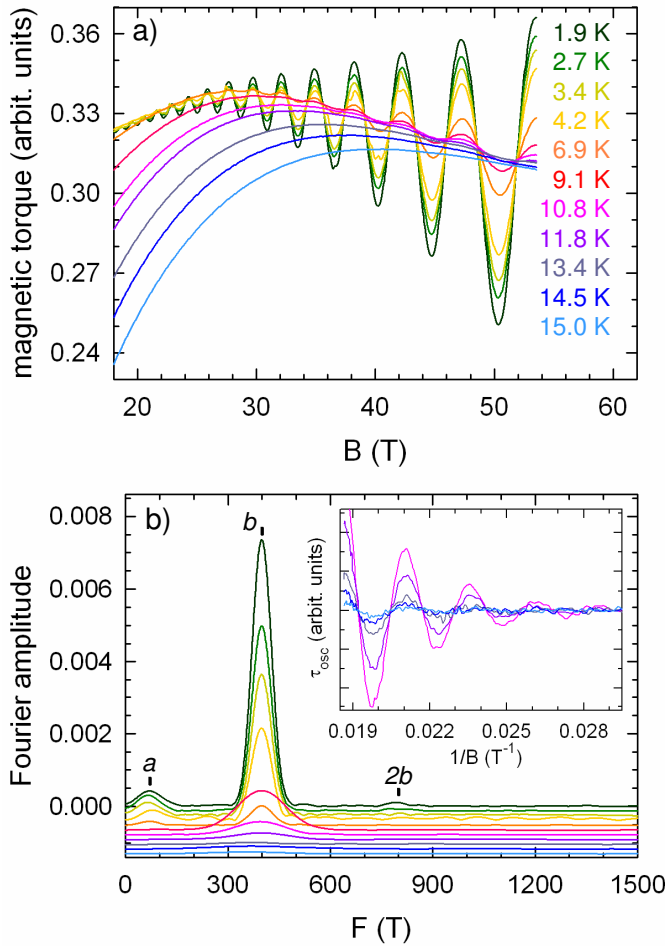


**Fig. 7.** (color on line) (a) Magnetic torque of  $\beta''$ -(ET)<sub>4</sub>(H<sub>3</sub>O)[Fe(C<sub>2</sub>O<sub>4</sub>)<sub>3</sub>].DCB at  $\theta = 29^\circ$ . (b) Fourier analyses deduced from data in (a). The field range is 30-53.5 T and 38-53.5 T below and above 9 K, respectively. The inset displays the oscillatory part of the data in (a) for temperatures above 10 K.

components with phase factors shifted by about 1/2, as can be observed in Fig. 6. More precisely, direct fittings in the considered temperature range yield  $\gamma_b = 0.1 \pm 0.1$  and  $0.55 \pm 0.10$ , respectively. In contrast, only one component, with  $\gamma_b = 0.15 \pm 0.10$ , can be observed in all the temperature range studied for  $\theta = 0$ . This behaviour is in line with the angle dependence of the spin zero damping factor (see

Eq. 5) for the  $b$  component at low temperature. Indeed, a good agreement between the angle dependence of the  $b$  component amplitude at 2 K and the LK formalism is observed. It yields  $\mu = 1.6 \pm 0.1$ , in rough agreement with the  $m_b$  value deduced from the low temperature part of the data, which suggests that  $g^*$  is close to 2. Therefore, not any zero can be observed below  $\theta = 50^\circ$ . The dephasing by about  $\pi$  in the high temperature range for  $\theta = 27^\circ$  could then be ascribed to a peculiar angle dependence of the QI phenomenon. Going further, it can be considered that the quantum interferometer responsible for the  $b$  component above  $\sim 6$  K is already present at the lowest temperature explored. In such a case, the Fourier amplitude should be the sum of the amplitudes linked to the SdH ( $A_{SdH}$ ) and QI ( $A_{QI}$ ) phenomena in all the temperature range studied, provided the phase factors are the same<sup>2</sup> which is the case for  $\theta = 0^\circ$ , as discussed above. The dashed line in Fig. 4 is the corresponding best fit of Eq. 1 to the data: a very good agreement is observed which indicates that the above hypothesis can be considered. The deduced effective mass is  $m_b^* = 1.6 \pm 0.1$  which is in excellent agreement with the above reported value of  $\mu$ .

The above data analysis suggests that a QI phenomenon accounts for the temperature dependence of the  $b$  com-

<sup>2</sup> Assuming the contribution of the  $b$  component to the oscillatory magnetoresistance ( $Y_b$ ) is given by  $Y_b = A_{SdH}\cos[2\pi(F_b/B+\gamma_{SdH})] + A_{QI}\cos[2\pi(F_b/B+\gamma_{QI})]$  yields  $Y_b = A_b\cos[2\pi(F_b/B+\gamma_b)]$  with  $A_b^2 = A_{SdH}^2 + A_{QI}^2 + 2A_{SdH}A_{QI}\cos[2\pi(\gamma_{SdH}-\gamma_{QI})]$  and  $\tan\gamma_b = [A_{SdH}\sin(2\pi\gamma_{SdH}) + A_{QI}\sin(2\pi\gamma_{QI})]/[A_{SdH}\cos(2\pi\gamma_{SdH}) + A_{QI}\cos(2\pi\gamma_{QI})]$ .

ponent amplitude. In the case where this hypothesis is valid, magnetization which as a thermodynamic parameter is only sensitive to the density of states should not reveal any contribution of QI. Torque data obtained for a field direction  $\theta = 29^\circ$  are displayed in Fig. 7(a). It can be remarked that  $F_{b-a}$  is not detected in dHvA spectra which could suggest that it corresponds to a QI path, as well, even though its effective mass is rather large ( $m^* = 1.0 \pm 0.1$ , see above). However, owing to the  $\mu_i$  value deduced from the angle dependence of the  $b$  SdH oscillations, this field direction yields the largest amplitude for this component. Oppositely, the  $b - a$  oscillations amplitude is strongly reduced, as evidenced in Fig. 3 for  $\theta = 27^\circ$ . Namely, the ratio  $A(b-a)/A(b)$  is decreased by a factor of 5 as  $\theta$  goes from 0 to  $29^\circ$ . In addition, dHvA oscillations are detected in a narrower field range than for SdH oscillations which broadens the Fourier peaks. Actually, only the  $a$ ,  $b$ , and  $2b$ , components can be detected in the Fourier analysis of the oscillatory part of the data (see Fig. 7(b)). In the framework of the LK theory, the oscillatory part of the magnetic torque  $\tau_{osc}$  can be expressed as [19,23]:

$$\tau_{osc} = B \tan \theta \sum_j T_j \sin[2\pi(\frac{F_j}{B} - \gamma_j)], \quad (8)$$

where  $T_j \propto R_{Tj} R_{Dj} R_{MBj} R_{Sj}$ . Examples of temperature dependence of the  $b$  oscillations amplitude are reported in Fig. 4. As displayed in Fig. 7(b), oscillations are detectable up to 15 K, i. e. at temperatures much higher than 6 K, at which QI oscillations start to mostly contribute to the magnetoresistance oscillations amplitude. In contrast to SdH data, no kink is observed for dHvA

oscillations. This behaviour corroborates the assumption that QI is responsible for the persistence of magnetoresistance oscillations at high temperature. The effective mass deduced from dHvA data in Fig. 4 corresponds to  $m_b^*(\theta = 0^\circ) = 1.5 \pm 0.1$  which is in good agreement with SdH data at low temperature. The question remaining to solve deals with the actual FS topology allowing both closed orbit and QI with the same frequency. In that respect, no decisive clue is observed since the main feature that could eventually account for FS reconstruction is a slight upturn of the zero-field resistance at low temperature [14].

The Dingle temperature deduced from dHvA data,  $T_D = 3.3 \pm 0.5$  K, is roughly a factor of two lower than for (NH<sub>4</sub>, Fe, C<sub>3</sub>H<sub>7</sub>NO) and (NH<sub>4</sub>, Cr, C<sub>3</sub>H<sub>7</sub>NO) [5,9]. Even though  $T_D$  can be significantly crystal dependent, it can be remarked that this value is in the same range as for (H<sub>3</sub>O, M, C<sub>5</sub>H<sub>5</sub>N), where M = Ga, Cr, Fe [7]. These rather high values are in line with the significant structural disorder observed in most of these compounds [11, 12,13]. According to Ref. [11] the disorder level is related to the ability of the solvent molecule to fill the cavities of the anion layer and is therefore linked to the solvent molecule size. More precisely, it has been inferred that the length of the solvent molecule along the  $b$  crystallographic axis is the pertinent parameter for the reduction of both the disorder level and the increase of the superconducting transition temperature [14]. However, owing to the rather poor correlation between the reported  $T_D$  values and the solvent molecule size (either volume or length), it can be

inferred that this latter parameter cannot alone account for the scattering rate deduced from quantum oscillations.

## 4 Summary and conclusion

SdH and dHvA oscillations spectra of the q-2D charge transfer salt  $\beta''$ -(ET)<sub>4</sub>(H<sub>3</sub>O)[Fe(C<sub>2</sub>O<sub>4</sub>)<sub>3</sub>]-C<sub>6</sub>H<sub>4</sub>Cl<sub>2</sub> reveal three main frequencies  $F_a = 74 \pm 5$  T,  $F_{b-a} = 272 \pm 5$  T and  $F_b = 348 \pm 3$  T. These frequencies are linked through the linear combination  $F_a + F_{b-a} = F_b$  that is consistent with a FS composed of three compensated closed orbits, as already reported for few other members of this family [5,9,17]. Effective masses,  $m_a^* = 0.85 \pm 0.10$ ,  $m_{b-a}^* = 1.0 \pm 0.1$  and  $m_b^* = 1.5 \pm 0.1$ , are in the same range as for the other salts of the family [5,6,7,8,9,17]. However, as for SdH spectra, the temperature dependence of the  $b$  component amplitude exhibits a kink at about 6 K, followed by a very weak variation. As a result, oscillations can be observed up to 32 K. This feature is not observed for dHvA oscillations (up to 15 K) which is consistent with a QI phenomenon arising from a quantum interferometer with a zero effective mass, having the same cross section as the closed orbit responsible for the  $b$  oscillations in the low temperature range. Both of them coexist, at least in the range 6 - 9 K for which two Fourier components with the frequency  $F_b$ , roughly in phase opposition, can be observed for  $\theta = 27^\circ$ , likely due to a different spin-dependent behaviour of the two contributions. In fact, coexistence of these two phenomena in all the temperature range studied can be considered. This result would be in line with the hypothesis of a quantum interferometer built on the  $b$  closed

orbit thanks to FS reconstruction at low temperature. Unfortunately, in the absence of a reliable knowledge of the FS topology at low temperature, this conclusion must be taken with caution.

Finally, the deduced Dingle temperature lies within the range of the values reported so far in the literature for the compounds of this family. No clear dependence of the scattering rate on the solvent molecule size can be inferred from the available data.

This work has been supported by FP7 I3 EuroMagNET II and by the French-Spanish exchange programm between CNRS and CSIC (number 18858).

## References

1. E. Coronado and P. Day, Chem. Rev. **104** (2004) 5419.
2. T. G. Prokhorova, S. S. Khasanov, L. V. Zorina, L. I. Buravov, V. A. Tkacheva, A. A. Baskakov, R. B. Morgunov, M. Gener, E. Canadell, R. P. Shibaeva and E. B. Yagubskii, Adv. Funct. Mater. **13** (2003) 403.
3. M. Kurmoo, A. W. Graham, P. Day, S. J. Coles, M. B. Hursthouse, J. L. Caulfield, J. Singleton, F. L. Pratt, W. Hayes, L. Ducasse and P. Guionneau, J. Am. Chem. Soc. **117** (1995) 12209.
4. A. D. Dubrovskii, N. G. Spitsina, L. I. Buravov, G. V. Shilov, O. A. Dyachenko, E. B. Yagubskii, V. N. Laukhin and E. Canadell, J. Mater. Chem. **15** (2005) 1248.
5. A. Audouard, V. N. Laukhin, L. Brossard, T. G. Prokhorova, E. B. Yagubskii and E. Canadell, Phys. Rev. B **69** (2004) 144523.

6. A. Bangura, A. Coldea, A. Ardavan, J. Singleton, A. Akutsu-Sato, H. Akutsu and P. Day, *J. Phys. IV France* **114** (2004) 285.
7. A. Coldea, A. Bangura, J. Singleton, A. Ardavan, A. Akutsu-Sato, H. Akutsu, S. S. Turner and P. Day, *Phys. Rev. B* **69** (2004) 085112.
8. A. Bangura, A. Coldea, J. Singleton, A. Ardavan, A. Akutsu-Sato, H. Akutsu, S. S. Turner and P. Day, *Phys. Rev. B* **72** (2005) 14543.
9. D. Vignolles, V. N. Laukhin, A. Audouard, T. G. Prokhorova, E. B. Yagubskii and E. Canadell, *Eur. Phys. J. B* **51** (2006) 53.
10. R. Rousseau, M. Gener and E. Canadell, *Adv. Func. Mater.* **14** 201 (2004).
11. S. S. Turner, P. Day, K. M. A. Malik, M. B. Hursthouse, S. J. Teat, E. J. MacLean, L. Martin and S. A. French, *Inorg. Chem.* **38** (1999) 3543.
12. S. Rashid, S. S. Turner, P. Day, J. A. K. Howard, P. Guionneau, E. J. L. McInnes, F. E. Mabbs, J. H. Clark, S. Firth and T. Briggs, *J. Mater. Chem.* **11** (2001) 2095.
13. H. Akutsu, A. Akutsu-Sato, S. S. Turner, D. Le Pevelen, P. Day, V. N. Laukhin, A.-K. Klehe, J. Singleton, D. A. Tocher, M. R. Probert and J. A. K. Howard, *J. Am. Chem. Soc.* **124** (2002) 12430.
14. L. Zorina, T. G. Prokhorova, S. Simonov, S. Khasanov, R. Shibaeva, A. Manakov, V. Zverev, L. Buravov and E. B. Yagubskii, *J. of Expt. and Theor. Phys.* **106** (2008) 347.
15. E. Ohmichi and T. Osada, *Rev. Sci. Inst.* **73** (2002) 3022.
16. C. Jaudet, D. Vignolles, A. Audouard, J. Levallois, D. LeBoeuf, N. Doiron-Leyraud, B. Vignolle, M. Nardone, A. Zitouni, R. Liang, D. A. Bonn, W. N. Hardy, L. Taillefer, and C. Proust, *Phys. Rev. Lett.* **100** (2008) 187005.
17. A. Audouard, V. N. Laukhin, J. Béard, D. Vignolles, M. Nardone, E. Canadell, T. G. Prokhorova and E. B. Yagubskii, *Phys. Rev. B* **74** (2006) 233104.
18. D. Vignolles, A. Audouard, V. N. Laukhin, J. Béard, E. Canadell, N. G. Spitsina and E. B. Yagubskii, *Eur. Phys. J. B* **55** (2007) 383.
19. D. Shoenberg, *Magnetic Oscillations in Metals* (Cambridge University Press, Cambridge, 1984).
20. R. W. Stark and C. B. Friedberg, *Phys. Rev. Lett.* **26** (1971) 556.
21. R. W. Stark and C. B. Friedberg, *J. Low Temp. Phys.*, **14** (1974) 111.
22. D. Vignolles, A. Audouard, L. Brossard, S. I. Pesotskii, R. B. Lyubovskii, M. Nardone, E. Haanappel and R. N. Lyubovskaya, *Eur. Phys. J. B*, **31** (2003) 53.
23. J. Wosnitza, *Fermi Surfaces of Low-dimensional Organic Metals and Superconductors* (Springer-Verlag, Berlin, Heidelberg, 1996).